A Generalized Power Supply Induced Jitter Model Based on Power Supply Rejection Ratio Response

Yin Sun, *Member, IEEE*, Jongjoo Lee, *Senior Member, IEEE*, and Chulsoon Hwang, *Senior Member, IEEE*

***Abstract*— In this work, a generalized power supply induced jitter (PSIJ) model is proposed. The PSIJ sensitivity is obtained based on the evaluation of driver power supply rejection ratio (PSRR) response. The voltage ripple at the driver output is transformed into driver output jitter with the slope of the switching edge. The time-averaged effect of power noise during the time range of driver propagation delay is also considered. The proposed model is applied to estimate the PSIJ sensitivity for typical inverter type of drivers and a low-voltage differential signaling (LVDS) type of current mode differential transmitter. Depending on the transistor working region in the driver, the PSIJ sensitivity frequency dependence could be dominated by either the propagation delay or the PSRR response. The accuracy of the predicted PSIJ sensitivity is verified by simulation. Reasonably good accuracy has been achieved in terms of both the magnitude and phase.**

***Index Terms*— Differential transmitter, inverter, power supply induced jitter (PSIJ), power supply rejection ratio (PSRR), propagation delay.**

I. Introduction

THE timing budget for today's I/O interfaces becomes tighter as the transition speed of I/O keeps increasing. Along with the continuously decreasing unit interval, the requirements for allowable jitter also become stricter and the jitter prediction becomes more important. In addition, with the scaling of power supply voltage levels and improving trans-conductance of drivers, the sensitivity of drivers to power supply induced delays has increased [1]. The power supply induced jitter (PSIJ) has become one of the major concerns for high-speed system [2]–[9].

For PSIJ characterization, the PSIJ sensitivity can be extracted from transistor-level simulation [5]. The obtained PSIJ sensitivity spectrum can be applied to calculate the total PSIJ if the power supply noise spectrum is known. The PSIJ sensitivity for inverter type of buffers has been widely studied [2], [5]–[8], as these buffers are frequently inserted in clock and timing circuits and the corresponding delays account for a large percentage of critical timing nets in the design [6]. However, there are not much discussion about PSIJ sensitivity of drivers that are not based on an inverter. The other type of drivers is also implemented in many designs [9] and the PSIJ sensitivity for these drivers is also important. For PSIJ sensitivity derivation, some treat the inverter type of buffers as voltage controlled delay line (VCDL) [6], [8] and the PSIJ sensitivity can be easily derived with the form of a sinc function. However, this delay-based method cannot be generalized for the other type of drivers, as the other type of drivers cannot be simply regarded as a VCDL. A numerical method is proposed to estimate PSIJ for a current mode differential driver using a root-finding approach by classical Newton's method [10], but the expression is not straightforward and the physical meaning is not clearly revealed. In addition, a statistical method based on the response surface model combined with Latin hypercube sampling (LHS) is used to model jitter in short pulse generation circuits [11]. However, the model is purely mathematical and lacks physical meanings. Some works have provided analytical method based on the piecewise transistor linear model using transient analysis [2], [7], [12]. The jitter is estimated as the ratio of the output voltage ripple versus the switching edge slope. However, the analytical derivation in the time domain is complicated and difficult to apply to other type of drivers.

In this article, a generalized PSIJ sensitivity model based on power supply rejection ratio (PSRR) response is proposed. The output voltage ripple to the power rail voltage ripple relationship could be easily established through the PSRR response in the frequency domain, allowing easier derivation while maintaining some physical insights. The proposed model is applied for a single-stage inverter, an inverter chain, and a voltage differential signaling (LVDS) type of current mode differential transmitter. The PSIJ sensitivity derivation is based on the frequency-domain PSRR response, slope of the switching edge, and the time-averaged effect of power noise in the time range of propagation delay. The obtained PSIJ sensitivity expressions are validated through comparison with transistor-level circuit simulation for both the magnitude and phase. Depending on the transistor working region in the driver, the frequency dependence of PSIJ sensitivity can be determined by different factors.

II. PSRR-Based PSIJ Sensitivity Model

Conceptually, the PSIJ sensitivity can be written as the ratio of the output time interval error (TIE) Δt to the voltage ripple level on the power rail ΔV_{dd}, when a single-frequency

Manuscript received October 26, 2020; revised February 27, 2021; accepted March 21, 2021. Date of publication April 26, 2021; date of current version June 4, 2021. This work was supported in part by the National Science Foundation under Grant IIP-1916535. *(Corresponding author: Yin Sun.)*

Yin Sun was with the Electromagnetic Compatibility (EMC) Laboratory, Missouri University of Science and Technology, Rolla, MO 65401 USA. She is now with Zhejiang Lab, Hangzhou 311121, China (e-mail: ysc26@mst.edu).

Jongjoo Lee is with the SK Hynix Inc., Bundang 463070, South Korea (e-mail: john.john@sk.com).

Chulsoon Hwang is with the Electromagnetic Compatibility (EMC) Laboratory, Missouri University of Science and Technology, Rolla, MO 65401 USA (e-mail: hwangc@mst.edu).

Color versions of one or more figures in this article are available at https://doi.org/10.1109/TVLSI.2021.3072799.

Digital Object Identifier 10.1109/TVLSI.2021.3072799

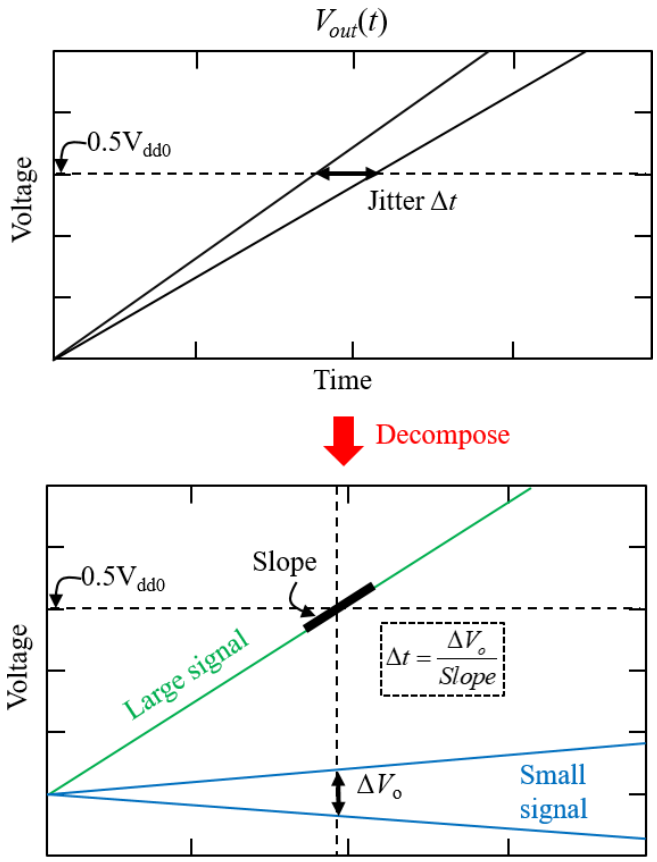

Fig. 1. Jitter derivation from decomposed multiple output voltage transition edges.

sinusoidal noise exhibits on the power rail. This ratio can be reformed into the ratio of PSRR to switching edge slope [13] as follows:

$$\frac{\Delta t}{\Delta V_{\rm dd}} = \frac{\Delta V_{\rm o}/\Delta V_{\rm dd}}{\Delta V_{\rm o}/\Delta t} = \frac{\rm PSRR}{\rm Slope} \tag{1}$$

where $\Delta V_{\rm o}$ is the variation in the output voltage. This concept can also be derived from the decomposed multiple output voltage transition edges as illustrated in Fig. 1. The two low-to-high transition edges are the minimum and maximum propagation delay cases corresponding to the maximum and minimum of a sinusoidal power voltage fluctuation, respectively. At half the nominal power rail voltage $V_{\rm dd0}$, the timing difference between the two edges is jitter Δt. The multiple output transition edges can be decomposed into a large signal portion, where the transition happens with power rail voltage $V_{\rm dd0}$, and a small-signal portion, which is introduced by the power rail voltage fluctuation [2], [3]. At half $V_{\rm dd0}$, the slope can be determined from the large-signal portion and the variation in the output voltage $\Delta V_{\rm o}$ can be extracted from the small-signal portion. The jitter can then be estimated as $\Delta t = \Delta V_{\rm o}/\rm Slope$.

The frequency-domain PSRR response PSRR(ω) can be separated into the peak value portion $\rm PSRR_p$ and the normalized frequency dependence portion $\rm PSRR'(\omega) = PSRR(\omega)/PSRR_p$. In low-frequency ranges where the voltage ripple period is much larger than the propagation delay, the power rail ripples affect the driver output noise in the same manner as a dc offset [2]. In these low-frequency ranges and dc condition, the PSRR is constant and has the peak value since it is determined only by the amplitude of the power rail noise. $\rm PSRR_p$ can be written as the ratio of output fluctuation to power rail voltage fluctuation at dc, $\Delta V_{\rm o}/\Delta V_{\rm dd}|_{\rm dc}$. The slope can be expressed as the ratio of output fluctuation to delay change at dc, $\Delta V_{\rm o}/\Delta t|_{\rm dc}$. Equation (1) can then be reformed as

$$\left|\frac{\rm PSRR(\omega)}{\rm Slope} = \frac{\rm PSRR_p \cdot PSRR'(\omega)}{\rm Slope}\right.$$
$$= \frac{\Delta V_{\rm o}/\Delta V_{\rm dd}|_{\rm DC}}{\Delta V_{\rm o}/\Delta t|_{\rm DC}}\rm PSRR'(\omega) = \left.\frac{\Delta t}{\Delta V_{\rm dd}}\right|_{\rm DC} PSRR'(\omega) \tag{2}$$

where ω is the angular frequency. Since the jitter is evaluated at half $V_{\rm dd0}$, it is a common practice to extract the slope of the transition edge near this voltage level [14], as illustrated in Fig. 2(a). By taking a small variation in the output voltage and recording the corresponding timing difference, the slope of the rising edge can be calculated. However, in practice, the rising edge is not a perfect straight line and the output edge slope during propagation delay time range will not be a constant. Applying the slope value read from the output edge near half $V_{\rm dd0}$ can lead to inaccurate PSIJ sensitivity results, as the slope effect during the entire propagation delay time range is neglected. To obtain a slope value that can give a better result for PSIJ sensitivity estimation, the slope is extracted from the driver delay change test under different power rail voltage levels at dc, as depicted in Fig. 2(b). With maximum power rail voltage level $V_{\rm dd,max}$, the corresponding propagation delay of the driver will be the smallest $T_{\rm pd,min}$. With minimum power rail voltage level $V_{\rm dd,min}$, the driver will exhibit a maximum propagation delay as $T_{\rm pd,max}$. The ratio of the variation in power voltage $\Delta V_{\rm dd}$ to the corresponding variation in propagation delay Δt is related to slope, as represented in the following equation:

$$\frac{\rm Slope}{\rm PSRR_p} = \left.\frac{\Delta V_{\rm dd}}{\Delta t}\right|_{\rm DC} = \frac{V_{\rm dd.\,max} - V_{\rm dd.\,min}}{T_{\rm pd,max} - T_{\rm pd,min}} \tag{3}$$

which is the inverse of the dc jitter sensitivity $(T_{\rm pd,max} - T_{\rm pd,min})/(V_{\rm dd,max} - V_{\rm dd,min})$.

As previously mentioned, the noise presented on the power rail will influence the output switching edge during the entire

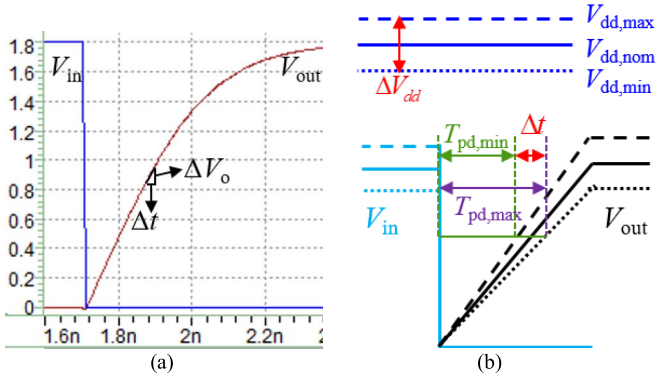

Fig. 2. Rising edge slope estimation. (a) Direct estimation. (b) From dc delay change test.

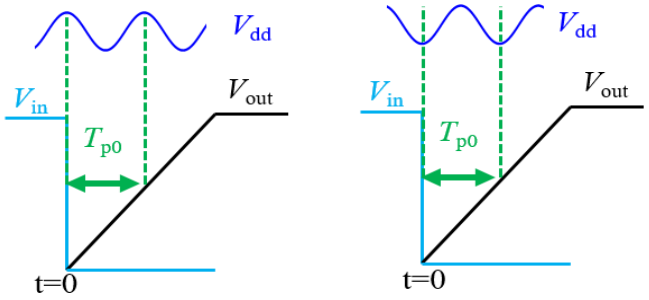

Fig. 3. Power noise time-averaged effect during propagation delay.

time range of the driver propagation delay T_{p0}, as illustrated in Fig. 3. In this study, it is assumed that the drivers work in the above-threshold region. In addition, the rise time of the input signal is assumed to be negligible [2], [14]. Moreover, the amplitude of power noise is small so the jitter magnitude is proportional to noise amplitude. Under these conditions, if the period of the sinusoidal noise on the power rail is the same as the propagation delay of the driver, regardless of the actual value of the power rail noise at the time when the output voltage is half V_{dd0}, the output switching edge delay time will not change. This is also true if the noise period is a multiple of the propagation delay. This is because the time-averaged effect of the noise at this specific frequency is zero during the time range of the propagation delay [2], [6]. For the PSIJ sensitivity derivation, this effect should be taken into consideration. For drivers working in the sub-threshold region, the jitter analysis is presented in [15] and will not be covered in this study.

Based on the above discussion, the PSIJ sensitivity formulation can be derived. Substituting (3) into (2) and taking the time harmonic form of PSRR(ω) for the time-averaged effect consideration, the PSIJ sensitivity is expressed as follows:

$$\text{PSIJ sensitivity}(\omega) = \int_0^{T_{p0}} \frac{\text{PSRR}(\omega)\cdot e^{j\omega t}}{\text{Slope}\cdot T_{p0}} dt = \frac{\text{PSRR}_p}{\text{Slope}} \text{PSRR}'(\omega) e^{j\frac{\omega}{2}T_{p0}} \text{sinc}\left(\frac{\omega}{2}T_{p0}\right). \quad (4)$$

The left-hand side of (4) indicates the jitter sensitivity transfer function and can be a complex number. From (4), it can be observed that the PSIJ sensitivity is related to the dc jitter sensitivity and the frequency dependence originates from the normalized PSRR response and the time-averaged effect-induced sinc function portion. This sinc function portion is also shown in previously derived expressions [6], [16].

In this work, the proposed model is applied for the PSIJ analysis for the three different drivers as shown in Fig. 4. For different type of drivers, the PSIJ sensitivity frequency dependencies are expected to be different. Since the driver PSIJ sensitivity frequency behavior is related to the PSRR response and the propagation delay, the different PSIJ sensitivity frequency behavior can be understood by the analysis of PSRR response and the equivalent *RC* delay of the circuit, as illustrated in Fig. 5.

The analysis for a single-stage inverter is shown in Fig. 5(a). The PMOS can be regarded as a resistor when looking at the rising edge case. The PSRR analysis is close to the analysis

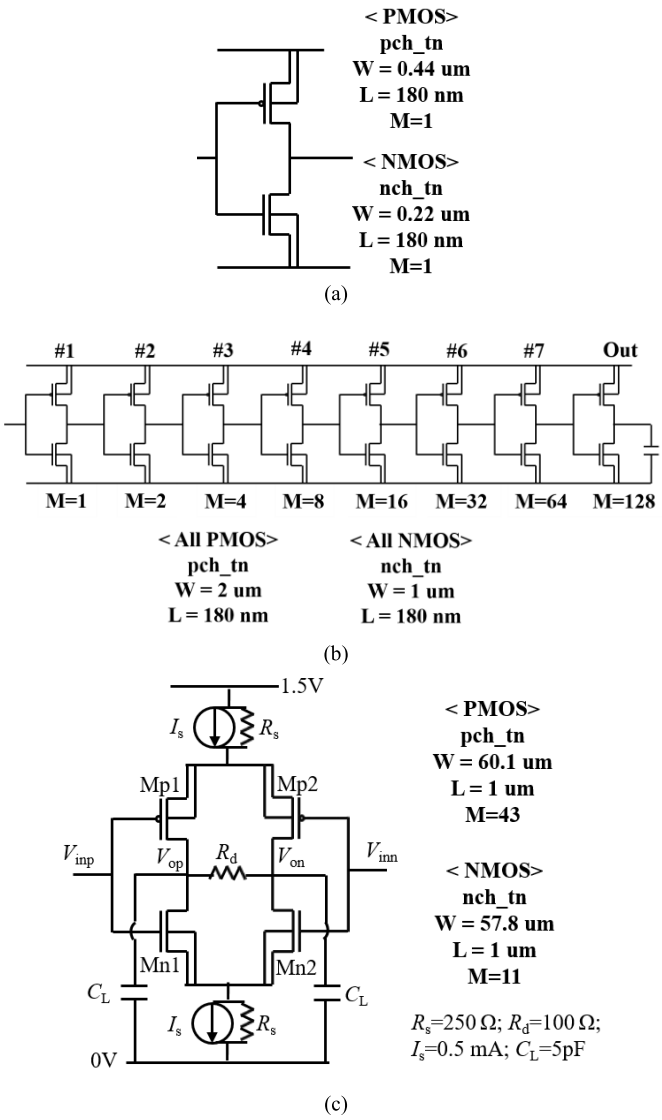

Fig. 4. Tested drivers. (a) Inverter. (b) Inverter chain. (c) Current mode differential driver.

for a first-order low-pass filter, with a cutoff frequency around $1/R_{op}C$, where R_{op} is the turn-on resistance of PMOS. For the output delay of the inverter, it can be roughly estimated as $R_{op}C$, and the corresponding frequency is the null frequency for the sinc function portion. In this case, the propagation-delay-related frequency roll-off is faster than the PSRR-related frequency roll-off. As a result, the PSIJ sensitivity frequency dependence is dominated by the propagation-delay-related time-averaged effect. For inverter chain, as the propagation delay is a linear accumulation of delay of each stage [7], the null frequency for the sinc function portion will be even smaller than the cutoff frequency of the PSRR response.

The analysis for current mode differential driver is shown in Fig. 5(b). For the designed driver, the transistors will have some amplification effects. For the simplest estimation, the PSRR analysis can be regarded as the analysis for a common gate amplifier. The cutoff frequency can be estimated as $1/g_m r_o R_s C$ [17], where g_m is the PMOS transconductance, r_o is the PMOS output resistance, and R_s is the

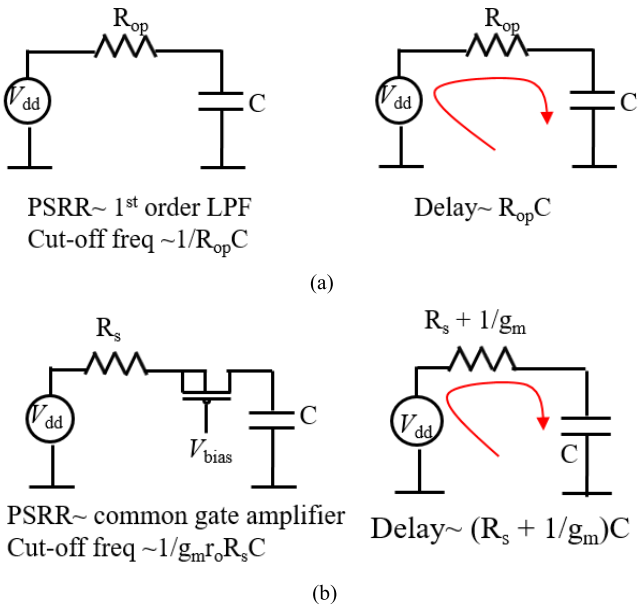

Fig. 5. Comparison of frequency dependence due to PSRR and propagation delay. (a) Inverter. (b) Differential driver.

current source resistance. On the other hand, for the delay estimation, the transistor can be regarded as a resistor with value of $1/g_{\mathrm{m}}$. So the propagation delay is roughly estimated as $(R_{\mathrm{s}} + 1/g_{\mathrm{m}})C$. In general, $g_{\mathrm{m}} r_{\mathrm{o}} R_{\mathrm{s}} C$ is larger than $(R_{\mathrm{s}} + 1/g_{\mathrm{m}})C$ [17]. In consequence, the PSRR response will have smaller cutoff frequency and the PSRR frequency dependence will roll off faster than the propagation-delay-related sinc function frequency dependence.

In summary, for drivers working in the deep triode region, since the transistor can be treated as a resistor, the PSRR response frequency roll-off tends to be slower than the propagation-delay-related frequency roll-off. In this case, the PSIJ sensitivity frequency dependence is dominated by the propagation-delay-related time-averaged effect. In addition, for drivers with multiple stages, as the total propagation delay is the accumulation of each single stage, the propagation-delay-related frequency roll-off tends to be faster than the PSRR-related frequency roll-off. The PSIJ sensitivity frequency dependence will also be dominated by the propagation delay. On the other hand, for drivers working in the linear region or the saturation region, as the transistor has some amplification effects, the PSRR frequency roll-off tends to be faster than the propagation-delay-related frequency roll-off. The PSIJ sensitivity frequency dependence will be dominated by the PSRR response portion.

III. Validation on Different Drivers

A. Inverter

The proposed PSRR-based PSIJ sensitivity model is first applied for a single-stage inverter. The design parameters for the single-stage inverter is shown in Fig. 4(a). To obtain the PSRR response of the inverter, the circuit needs to be set to a proper dc status. For a single-stage inverter, the power rail noise voltage will mainly influence the low-to-high transition. If the input switching edge transition time is assumed to be

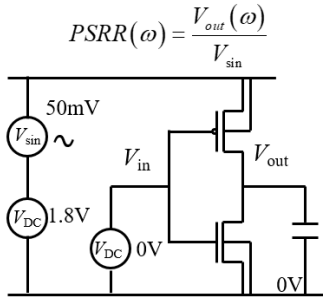

Fig. 6. PSRR simulation test for a single-stage inverter.

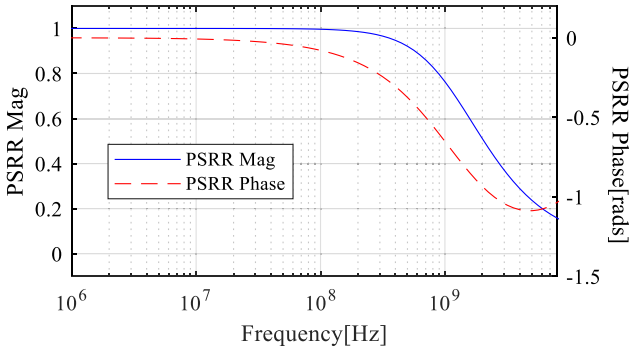

Fig. 7. PSRR simulation result for a single-stage inverter.

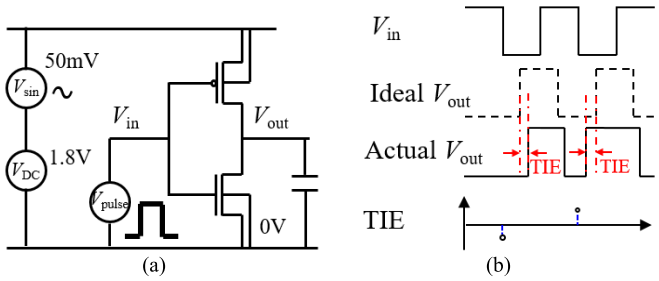

Fig. 8. Simulation setup for jitter extraction. (a) Setup. (b) Extraction of TIE sequence.

negligible, when the output transits from low to high, the input will always be low. For the PSRR simulation, the input is set to zero as plotted in Fig. 6. The nominal power rail voltage for this inverter is 1.8 V and a sinusoidal source with 50-mV amplitude is served as the noise source. The load capacitance for the test is set to 20 fF. By conducting ac simulation and obtaining the ratio of the output voltage to the amplitude of sinusoidal noise, the PSRR response for the output rising edge case is obtained.

The simulated PSRR magnitude and phase for the inverter are shown in Fig. 7. At low-frequency range, the magnitude of PSRR is one, and at higher frequency range, the PSRR begins to fall off. This is because for the PSRR simulation setup, the NMOS is set to off and PMOS is in the linear region. At low-frequency range, the PMOS is regarded as a resistor and the loading capacitor can be treated as open. As a result, the output will have the same amplitude as the input. With the increase in the frequency, the capacitor will start to take effect and the output voltage will begin to fall off.

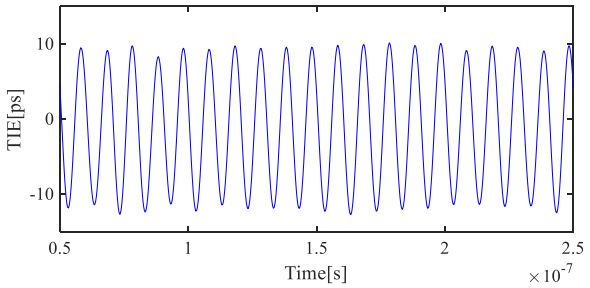

Fig. 9. Extracted TIE sequence for the case with 100-MHz power noise.

To validate the proposed PSIJ sensitivity expression (4), Hspice simulation is conducted to obtain the reference PSIJ sensitivity values at different frequencies. The simulation setup for jitter extraction is depicted in Fig. 8(a). To obtain both the magnitude and phase information, the TIE sequence is extracted as illustrated in Fig. 8(b). The TIE is calculated by subtracting the actual output edge switching time from the ideal output edge switching. The obtained TIE value for each edge is plotted in the time domain with respect to the input edge switching time; as in the derivation of (4), the time of input edge switching is treated as zero during the integration process. The extracted TIE sequence for the case with 100-MHz power noise is shown in Fig. 9, from which the magnitude and phase of the PSIJ can be acquired. The comparison of the PSIJ sensitivity magnitude and phase results obtained from the PSRR-based model and Hspice simulation is shown in Fig. 10(a) and (b), respectively. The proposed PSIJ sensitivity model exhibits reasonably good estimation accuracy compared with the simulation results.

B. Inverter Chain

Equation (4) can also be applied for inverter chain PSIJ sensitivity analysis with proper modification on the PSRR response and slope portion. Since each stage in the inverter chain will have their own PSRR response and slope, which will all contribute to the total PSIJ, the form of (4) needs to be adjusted accordingly. For the inverter chain, the total PSIJ at the final output stage can be obtained from the linear accumulation of local PSIJ at each stage [7], as illustrated in Fig. 11. Since the switching edge directions are opposite for the odd and even number stages in the inverter chain, the polarity of induced jitter for the adjacent stages will be opposite, as the slopes of rising and falling edges are opposite in sign.

The design parameters for the tested inverter chain are shown in Fig. 4(b). The loading capacitance at the last stage is 10 fF. This is an eight-stage inverter chain where each stage size is increased by the same factor of 2. For each stage, PMOS is twice the size of NMOS. For the inverter chain designed in this fashion, besides the last output stage, the propagation delay of #1 to #7 stages will be almost the same and the rising and falling edge propagation delays will also be very similar. In addition, the PSRR responses of #1 to #7 stages are almost identical.

For each stage, the PSRR response for the rising edge case can be obtained by setting the input of each stage as low. The PSRR response for the falling edge case can be extracted by setting the input of each stage high. The PSRR response of each stage for both the rising and falling edges in the inverter chain is summarized in Fig. 12. The PSRR response for #1 to #7 stages is identical and is plotted in Fig. 12(a) while the last stage PSRR response is shown in Fig. 12(b).

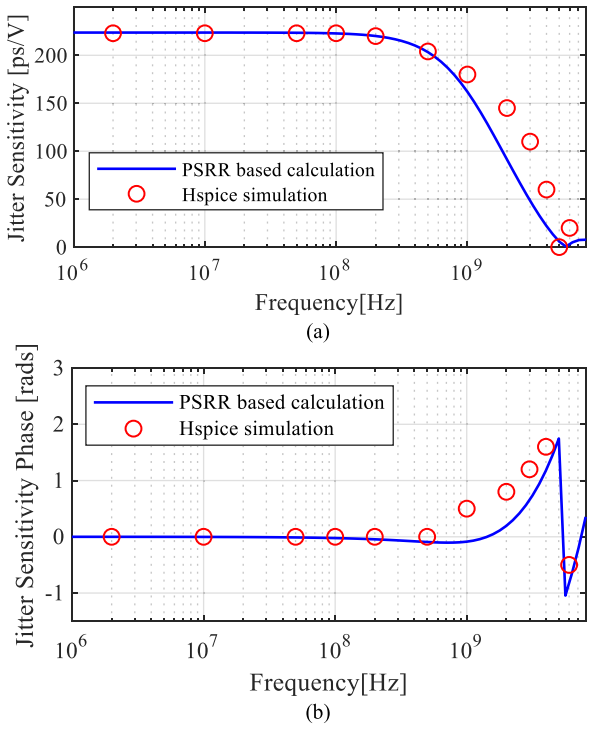

Fig. 10. Single-stage inverter PSIJ sensitivity results' comparison between the PSRR-based model and Hspice simulation. (a) Magnitude. (b) Phase.

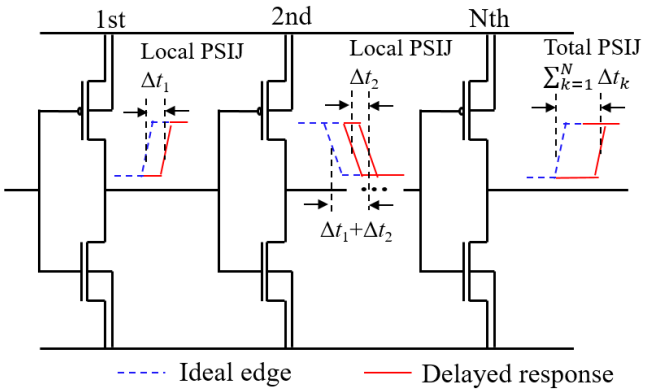

Fig. 11. Inverter chain total PSIJ as sum of each stage local PSIJ.

For the inverter chain output rising edge case, the total jitter can be calculated by the linear summation of the local PSIJ as follows:

$$\left.\frac{\mathrm{PSRR_p}}{\mathrm{Slope}}\right|_{\#1-\#7}\left(3\cdot \mathrm{PSRR}'(\omega)_{\mathrm{rise}}-4\cdot \mathrm{PSRR}'(\omega)_{\mathrm{fall}}\right)+\left.\frac{\mathrm{PSRR_p}}{\mathrm{Slope}}\right|_{V_{\mathrm{out}}}\mathrm{PSRR}'(\omega)_{\mathrm{rise}}\Big|_{V_{\mathrm{out}}}=\left.\frac{\mathrm{PSRR_p}}{\mathrm{Slope}}\right|_{\#1-\#7}A'_{R\_\#1-\#7}(\omega)+\left.\frac{\mathrm{PSRR_p}}{\mathrm{Slope}}\right|_{V_{\mathrm{out}}}A'_{R\_V_{\mathrm{out}}}(\omega). \quad (5)$$

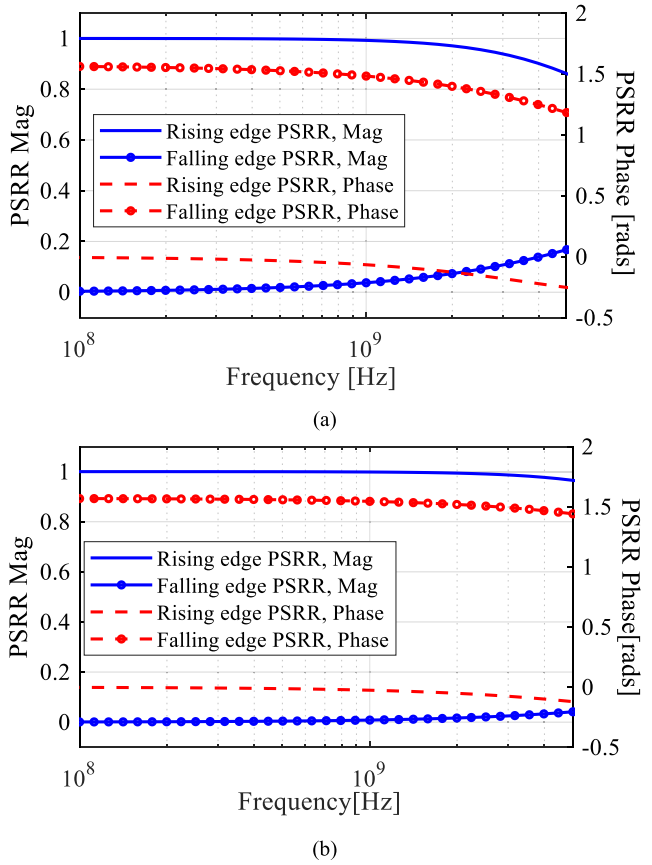

Fig. 12. PSRR for each stage in inverter chain. (a) #1–#7 stages. (b) Output stage.

The local PSIJ of each stage is expressed as the form of the dc performance portion multiplied with the normalized frequency dependence portion as shown in (2). Since the #1 to #7 stages share the same PSRR and rising/falling edge characteristics, the dc performance portion is the same and is written as $\mathrm{PSRR_p/Slope}|_{\#1-\#7}$. On the other hand, the dc performance portion for the final stage is different and is expressed as $\mathrm{PSRR_p/Slope}|_{V_{\mathrm{out}}}$. For the case where the final output stage is rising, there will be four falling edges and three rising edges in the previous seven stages. All the rising edge stages will have the same normalized PSRR frequency dependence portion $\mathrm{PSRR}'(\omega)_{\mathrm{rise}}$, while all the falling edge stages will have the same normalized PSRR frequency dependence portion $\mathrm{PSRR}'(\omega)_{\mathrm{fall}}$. The normalized PSRR frequency dependence portion for the last output stage is $\mathrm{PSRR}'(\omega)_{\mathrm{rise}}|_{V_{\mathrm{out}}}$. The signs of local PSIJs for the adjacent stages are opposite and are explicitly expressed since the slope is treated as a magnitude value. For simplification, the normalized frequency dependence portion of the #1 to #7 stages is written as $A'_{R\_\#1-\#7}(\omega)$, and for the last stage, the normalized frequency dependence portion is expressed as $A'_{R\_V_{\mathrm{out}}}(\omega)$.

The dc performance portion can also be estimated by the dc delay change test. The dc performance portions for the #1 to #7 stages can be evaluated together. By recording the dc delay change at the #7 stage of the inverter chain, the dc jitter sensitivity for the stages from #1 to #7 is written as $(T_{\mathrm{pd,max}} - T_{\mathrm{pd,min}})/(V_{\mathrm{dd,max}} - V_{\mathrm{dd,min}})|_{\#1-\#7}$. Since the PSRR response for the falling edge case is zero at dc, the dc jitter sensitivity is determined by the three rising edge stages and it can be concluded as follows:

$$\left.\frac{\mathrm{PSRR_p}}{\mathrm{Slope}}\right|_{\#1-\#7} = \left.\frac{T_{\mathrm{pd\,max}} - T_{\mathrm{pd\,min}}}{V_{\mathrm{dd\,max}} - V_{\mathrm{dd\,min}}}\right|_{\#1-\#7} \Big/ 3. \tag{6}$$

The dc performance portion for the last stage can be extracted by isolating this stage and treated as a single-stage inverter, keeping the original loading capacitance. The dc performance portion is estimated as the dc jitter sensitivity of the output stage $(T_{\mathrm{pd,max}} - T_{\mathrm{pd,min}})/(V_{\mathrm{dd,max}} - V_{\mathrm{dd,min}})|_{V_{\mathrm{out}}}$, as presented in the following equation:

$$\left.\frac{\mathrm{PSRR_p}}{\mathrm{Slope}}\right|_{V_{\mathrm{out}}} = \left.\frac{1}{\mathrm{Slope}}\right|_{V_{\mathrm{out}}} = \left.\frac{T_{\mathrm{pd\,max}} - T_{\mathrm{pd\,min}}}{V_{\mathrm{dd\,max}} - V_{\mathrm{dd\,min}}}\right|_{V_{\mathrm{out}}}. \tag{7}$$

As all the stages in the inverter chain are consecutive in time, the time-averaged effect of power rail noise should be considered in the propagation delay time range of the entire chain. Based on the above analysis, the application form of (4) for the inverter chain rising edge case is as follows:

$$\begin{aligned}&\mathrm{PSIJ\ sensitivity}(\omega)\\ &= \left[\begin{array}{l}\left.\dfrac{\mathrm{PSRR_p}}{\mathrm{Slope}}\right|_{\#1-\#7} A'_{R\_\#1-\#7}(\omega)\\ +\left.\dfrac{\mathrm{PSRR_p}}{\mathrm{Slope}}\right|_{V_{\mathrm{out}}} A'_{R\_V_{\mathrm{out}}}(\omega)\end{array}\right] e^{j\frac{\omega}{2}T_{pR0}} \sin c\left(\frac{\omega}{2}T_{pR0}\right)\end{aligned} \tag{8}$$

where T_{pR0} is the inverter chain propagation delay for the rising edge case. The PSIJ sensitivity formulation for the falling edge case can be derived similarly.

The obtained PSIJ sensitivity expressions for the rising and falling edge cases are validated using Hspice simulation. For rising edge, the comparison results of the PSRR-based model and Hspice simulation for PSIJ sensitivity magnitude and phase are plotted in Fig. 13(a) and (b), respectively. For falling edge, the comparison results of PSRR-based model and Hspice simulation for PSIJ sensitivity magnitude and phase are plotted in Fig. 14(a) and (b), respectively. The proposed model can estimate the inverter chain PSIJ sensitivity with reasonably good accuracy for both the magnitude and phase.

C. Current Mode Differential Driver

For current mode differential driver PSIJ sensitivity analysis, (4) can also be applied with proper modification on the PSRR response and slope portion. The PSRR response and slope of both the positive node and negative node need to be considered for PSIJ analysis. Since the slope of the positive node and negative node may be different, if only differential output PSRR response and slope is considered, the effect of the different slope in the positive and negative node to the PSIJ will be missed.

The design parameters for the current mode differential driver are shown in Fig. 4(c). The nominal power rail voltage is 1.5 V. The voltage levels for the single-ended output are designed to be 0.625 V for the low state and 0.875 V for the high state. The differential output swing will be 500 mV.

To obtain the PSRR response of the current mode differential driver, the circuit needs to be set to a proper dc status,

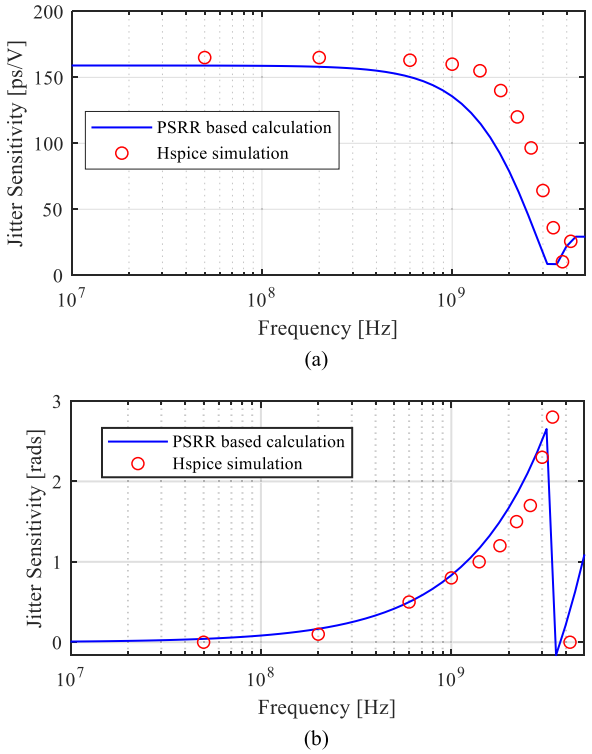

Fig. 13. Inverter chain rising edge PSIJ sensitivity results' comparison between the PSRR-based model and Hspice simulation. (a) Magnitude. (b) Phase.

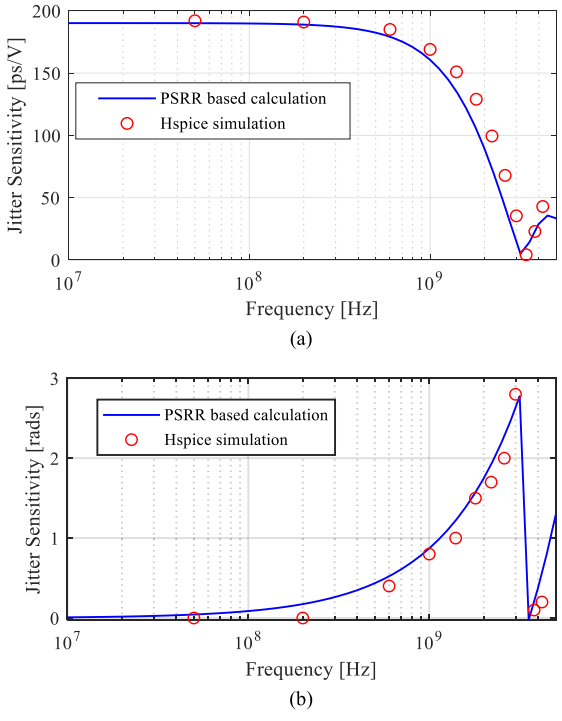

Fig. 14. Inverter chain falling edge PSIJ sensitivity results' comparison between the PSRR-based model and Hspice simulation. (a) Magnitude. (b) Phase.

as the input switching time is assumed to be negligible. The differential driver is switching between two dc statuses. For the case where the positive side input is low and the negative side

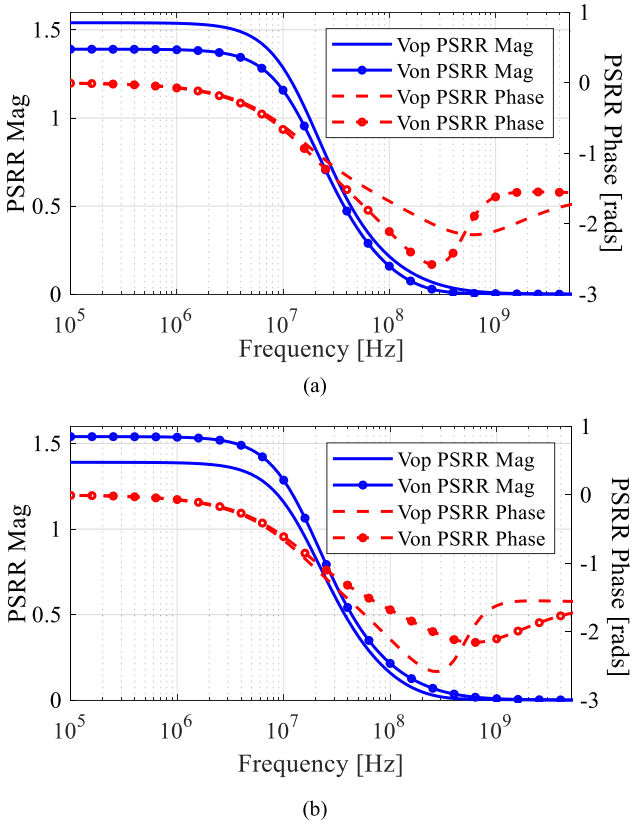

Fig. 15. PSRR of differential driver. (a) Positive input low, negative input high. (b) Positive input high, negative input low.

input is high, the magnitude and phase of the PSRR response are plotted in Fig. 15(a). For the case where the positive side input is high and the negative side input is low, the magnitude and phase of the PSRR response are plotted in Fig. 15(b). At a fixed dc status, the PSRR response for the positive and negative side is different. It should be noted that even though the PSRR response will change for the positive and negative side outputs when the dc status changes, eventually only two PSRR responses will be obtained, as Mp1 and Mp2 are the same and Mn1 and Mn2 are also the same. The PSRR response with larger value is denoted as $\text{PSRR}_{\text{nl}} = V_{\text{nl}}/V_{\text{sin}}$, where V_{sin} is the amplitude of the power rail noise. The PSRR response with smaller value is written as $\text{PSRR}_{\text{ns}} = V_{\text{ns}}/V_{\text{sin}}$.

The process to derive the differential TIE from PSRR response is illustrated in Fig. 16. The positive and negative node outputs with ideal power voltage are denoted as OP and ON, respectively. The voltage value for the low and high states is denoted as V_2 and V_1, respectively. The crossing time location of OP and ON under the nominal power voltage is denoted as t_{c}. The crossing voltage level at t_{c} is represented as V_{cross}. When the power voltage is increased, the changed positive and negative node outputs are indicated as OP′ and ON′, respectively. The difference between the new crossing time location t_{c}' and the original t_{c} is the differential output TIE. At the original t_{c}, OP′ will increase to V_{pnx} while ON′ will increase to V_{nnx}. The OP′ and ON′ crossing point, OP′ and t_{c} crossing point, as well as ON′ and t_{c} crossing

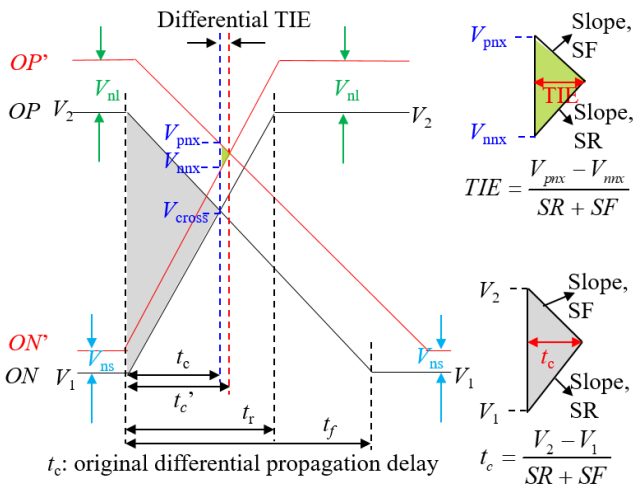

Fig. 16. Differential driver output TIE analysis illustration.

point have formed a triangle. The length of the triangle vertical edge is $V_{\text{pnx}} - V_{\text{nnx}}$ and differential TIE will be the height at this edge. The slope of the other two edges in the triangle is SR and SF, which are the magnitude of the rising and falling edge slope. From basic geometry theory, the differential TIE can be calculated as $(V_{\text{pnx}} - V_{\text{nnx}})/(\text{SR} + \text{SF})$. For simplicity, the SR and SF are assumed to be obtained under nominal power voltage. Similarly, the original crossing time t_c can be expressed as $(V_2 - V_1)/(\text{SR} + \text{SF})$. From this analysis, it is clearly shown that the differential TIE is related to the PSRR response and the rising/falling edge slopes.

V_{nnx} can be estimated as

$$V_{\text{nnx}} = V_{\text{cross}} + V_{\text{ns}} + V_{\text{nl}}\frac{t_c}{t_r} = V_{\text{cross}} + V_{\text{ns}} + V_{\text{nl}}\frac{\text{SR}}{\text{SR} + \text{SF}}. \quad (9)$$

When the power rail voltage is increased, before transition, ON′ will increase by V_{ns} compared with ON. After transition, for the flipped dc status, ON′ will increase by V_{nl}, compared with ON. During the transition, the negative node rising edge slope will also increase due to the PSRR response. At the original crossing time t_c, the voltage increase due to the increase in the rising edge slope is estimated as $V_{\text{nl}}(t_c/t_r)$, where t_r is the time when the negative node output changes from V_1 to V_2 and can be written as $(V_2 - V_1)/\text{SR}$. Plus the initial increase V_{ns}, V_{nnx} will be $V_{\text{cross}} + V_{\text{ns}} + V_{\text{nl}}(t_c/t_r)$.

A similar analysis is carried out for OP′ and V_{pnx} is expressed as follows:

$$V_{\text{pnx}} = V_{\text{cross}} + V_{\text{nl}} + V_{\text{ns}}\frac{t_c}{t_f} = V_{\text{cross}} + V_{\text{nl}} + V_{\text{ns}}\frac{\text{SF}}{\text{SR} + \text{SF}}. \quad (10)$$

Plugging V_{pnx} and V_{nnx} values in the differential TIE expression, normalizing to the amplitude of power rail noise, extracting the dc performance portion, and considering the time-averaged effect, the application form of (4) for the current

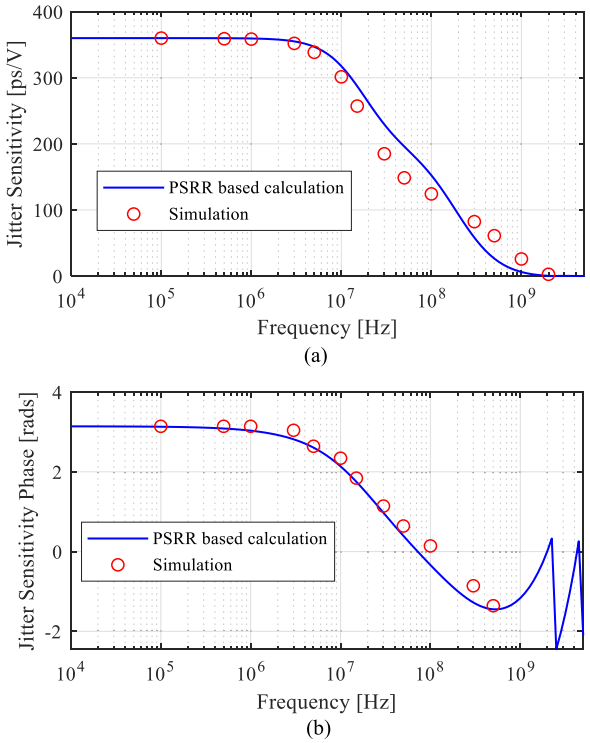

Fig. 17. Differential transmitter PSIJ sensitivity results' comparison between the PSRR-based model and Hspice simulation. (a) Differential output PSIJ magnitude. (b) Differential output PSIJ phase.

mode differential driver is derived as follows:

$$\begin{aligned}&\text{PSIJ sensitivity}(\omega)\\ &= \frac{\text{PSRR}_{\text{p}}}{\text{SF} + \text{SR}}\left(\begin{array}{l}\left(1 - \dfrac{\text{SR}}{\text{SR} + \text{SF}}\right)\text{PSRR}'_{\text{nl}}(\omega)\\ -\left(1 - \dfrac{\text{SF}}{\text{SR} + \text{SF}}\right)\text{PSRR}'_{\text{ns}}(\omega)\end{array}\right)\\ &\quad \times e^{j\frac{\omega}{2}T_{\text{p0}}}\sin c\left(\frac{\omega}{2}T_{\text{p0}}\right).\end{aligned} \quad (11)$$

T_{p0} is the differential output propagation delay. The dc performance portion is estimated with the differential output dc jitter sensitivity as

$$\frac{\text{PSRR}_{\text{p}}}{\text{SF} + \text{SR}} = \left|\frac{T_{\text{pd max}} - T_{\text{pd min}}}{V_{\text{dd max}} - V_{\text{dd min}}}\right|. \quad (12)$$

The normalized PSRR frequency dependence portions are PSRR'_{nl} and PSRR'_{ns} for PSRR_{nl} and PSRR_{ns}, respectively.

From (11), the influence of PSRR and transition edge slope of the positive and negative nodes can be evaluated. If the PSRR of the negative node and positive node is the same, and the magnitude of SR and SF is also the same, the differential TIE should be zero. If the PSRR responses are the same but the SR and SF are different, the differential TIE will appear and is proportional to $\text{PSRR}(\text{SR} - \text{SF})/(\text{SR} + \text{SF})^2$. If the slopes are the same but the PSRR responses are different, the differential TIE will also exist and is proportional to $0.5(\text{PSRR}_{\text{nl}} - \text{PSRR}_{\text{nl}})/(2\ \text{Slope})$.

The PSIJ sensitivity expression for the current mode differential driver is also validated by comparison with the Hspice

simulation results. The PSIJ sensitivity magnitude and phase are plotted in Fig. 17(a) and (b), respectively. The results from the PSRR-based calculation match reasonably well with the one obtained from transistor circuit simulation.

IV. Conclusion

The PSIJ sensitivity model based on PSRR response is derived and validated using Hspice simulation. The obtained PSIJ sensitivity formulations contain both the magnitude and phase information. The proposed PSIJ sensitivity model can be generalized for the PSIJ study of different type of drivers. In general, the PSIJ sensitivity for different type of drivers is related to the PSRR response, transition edge slope, and propagation delay. With the proposed model, the factors influencing the PSIJ sensitivity behavior for different type of drivers can be clearly identified.

References

[1] L. H. Chen, M. Marek-Sadowska, and F. Brewer, "Buffer delay change in the presence of power and ground noise," *IEEE Trans. Very Large Scale Integr. (VLSI) Syst.*, vol. 11, no. 3, pp. 461–473, Jun. 2003.

[2] C. Hwang, J. Kim, B. Achkir, and J. Fan, "Analytical transfer functions relating power and ground voltage fluctuations to jitter at a single-ended full-swing buffer," *IEEE Trans. Compon., Packag., Manuf. Technol.*, vol. 3, no. 1, pp. 113–125, Jan. 2013.

[3] Y. Sun, J. Kim, and C. Hwang, "Jitter-aware target impedance," in *Proc. IEEE Int. Symp. Electromagn. Compat.*, Jul. 2019, pp. 217–222.

[4] Y. Sun, J. Kim, M. Ouyang, and C. Hwang, "Improved target impedance concept with jitter specification," *IEEE Trans. Electromagn. Compat.*, vol. 62, no. 4, pp. 1534–1545, Aug. 2020.

[5] H. Lan *et al.*, "Power supply noise induced jitter in a 6.4 Gbps/link memory interface system," presented at the Design Conf., Santa Clara, CA, USA, 2012.

[6] X. J. Wang and T. Kwasniewski, "Propagation delay-based expression of power supply-induced jitter sensitivity for CMOS buffer chain," *IEEE Trans. Electromagn. Compat.*, vol. 58, no. 2, pp. 627–630, Apr. 2016.

[7] H. Kim, J. Kim, J. Fan, and C. Hwang, "Precise analytical model of power supply induced jitter transfer function at inverter chains," *IEEE Trans. Electromagn. Compat.*, vol. 60, no. 5, pp. 1491–1499, Oct. 2018.

[8] Y. Shim, J. Lee, and J. Kim, "Fast, precise and broadband modelling of induced clock jitter by SSN coupling," presented at the Design Conf., Santa Clara, CA, USA, 2012.

[9] G. Mandal and P. Mandal, "Low power LVDS transmitter with low common mode variation for 1GB/s-per pin operation," in *Proc. IEEE Int. Symp. Circuits Syst. (ISCAS)*, vol. 1, May 2004, pp. 1120–1123.

[10] J. N. Tripathi and F. G. Canavero, "An efficient estimation of power supply-induced jitter by numerical method," *IEEE Microw. Wireless Compon. Lett.*, vol. 27, no. 12, pp. 1050–1052, Dec. 2017.

[11] J. Sun, P. Wang, and H. Zhang, "Reducing power-supply and ground noise induced timing jitter in short pulse generation circuits," in *Proc. IEEE Symp. Electromagn. Compat. Signal Integrity*, Mar. 2015, pp. 17–21.

[12] J. N. Tripathi, R. Achar, and R. Malik, "Efficient modeling of power supply induced jitter in voltage-mode drivers (EMPSIJ)," *IEEE Trans. Compon., Packag., Manuf. Technol.*, vol. 7, no. 10, pp. 1691–1701, Oct. 2017.

[13] T. Pialis and K. Phang, "Analysis of timing jitter in ring oscillators due to power supply noise," in *Proc. Int. Symp. Circuits Syst. (ISCAS)*, vol. 1, May 2003, pp. 1–4.

[14] J. Kim *et al.*, "Analytical expressions for transfer function of supply voltage fluctuation to jitter at a single-ended buffer," in *Proc. IEEE Int. Symp. Electromagn. Compat.*, Aug. 2011, pp. 422–427.

[15] P. Corsonello, F. Frustaci, and S. Perri, "Power supply noise in accurate delay model for the sub-threshold domain," *Integration*, vol. 50, pp. 127–136, Jun. 2015.

[16] X. Wang, "Reduction of power supply induced jitter with applications to DDR controllers," Ph.D. dissertation, Dept. Electron., Carleton Univ., Ottawa, ON, Canada, 2016.

[17] A. S. Sedra, D. E. A. S. Sedra, K. C. Smith, and K. C. Smith, *Microelectronic Circuits*. New York, NY, USA: Oxford Univ. Press, 1998.

Yin Sun (Member, IEEE) received the B.S. degree in micro-electronics from Fudan University, Shanghai, China, in 2013, the M.S. degree in electrical and computer engineering from the Hong Kong University of Science and Technology (HKUST), Hong Kong, China, in 2016, and the Ph.D. degree in electrical engineering with the Electromagnetic Compatibility (EMC) Laboratory, Missouri University of Science and Technology (formerly University of Missouri-Rolla), Rolla, MO, USA, in 2020.

She is currently with the Zhejiang Lab, Hangzhou, China, as a Research Fellow. Her research interests include radio frequency interference in mobile devices, EMI source modeling and prediction, power-supply-induced jitter in I/O buffer, power distribution network target impedance design, signal/power integrity in high-speed digital systems, and acoustic noise in multilayer ceramic capacitors.

Jongjoo Lee (Senior Member, IEEE) received the M.S. and Ph.D. degrees in electrical engineering from the Korea Advanced Institute of Science and Technology (KAIST), Daejeon, Korea, in 1997 and 2001, respectively. His doctorial dissertation demonstrated the world-first development of photoconductive vectorial electric near-field probes using micromachining for transient mapping of picosecond electric-pulse propagation phenomena.

In 2002, he joined the Package team, Memory division, Samsung Electronics, Hwasung, South Korea, where he had developed the SI/PI co-simulation method used worldwide until now and the high-performance and high-density stack-package solutions, as the SI/PI leader. After leading EMI TF at the DRAM design team from 2009 to 2010, he was appointed to the Flash Solution development team, where he had directed the design and development of SSD hardwares, board design-guides for mobile memory customers, and the SI/Phy/EMC of NAND-storage devices until 2018. He was a Visiting Scholar at Shanghai Jiao Tong University, Shanghai, China, and Missouri S&T, Rolla, MO, USA, in 2015 and 2019, respectively. In 2020, he joined the SK Hynix, Bundang, South Korea, where he is currently the Head of Solution Design and Integration group. His current research interests include SI/PI/EMC and co-design and integration of device to system. He has been a listee of international biographical reference books since 2008. He has authored more than 100 patents and articles.

Chulsoon Hwang (Senior Member, IEEE) received the B.S., M.S., and Ph.D. degrees in electrical engineering from the Korea Advanced Institute of Science and Technology (KAIST), Daejeon, South Korea, in 2007, 2009, and 2012, respectively.

He was with Samsung Electronics, Suwon, South Korea, as a Senior Engineer from 2012 to 2015. In July 2015, he joined the Missouri University of Science and Technology (formerly University of Missouri-Rolla), Rolla, MO, USA, where he is currently an Assistant Professor. His research interests include RF desense, signal/power integrity in high-speed digital systems, EMI/EMC, hardware security, and machine learning.

Dr. Hwang was a recipient of the AP-EMC Young Scientist Award, the Google Faculty Research Award, and Missouri S&T's Faculty Research Award. He was a co-recipient of the IEEE EMC Best Paper Award, the AP-EMC Best Paper Award, and a two-time co-recipient of the DesignCon Best Paper Award.